



Machine Learning Implementation on Wind Speed Prediction

Akin ILHAN*

¹ Department of Energy Systems Engineering, Faculty of Engineering and Natural Sciences, Ankara Yildirim Beyazit University, 06010, Ankara, Turkey, ORCID ID: 0000-0003-3590-5291

*(ailhan@ybu.edu.tr) Email of the corresponding author

Abstract – In this study, the measured hub-height wind speed of a wind turbine is forecasted using machine learning. Accordingly, the wind speed data has been obtained from an installed wind turbine of a wind power plant that is located in the Republic of Kosovo. A cumulative of 2,000 wind speed data has been used in historical time-series predictions performed by long-short term memory, adaptive neuro-fuzzy inference system with fuzzy c-means (FCM), subtractive clustering (SC), and grid partitioning (GP). The results of 102 computed models have indicated that the best wind speed predictions have been obtained during the utilization of the ANFIS-SC algorithm. The accuracy of the predictions has been evaluated considering the mean absolute error (MAE), root mean square error (RMSE), as well as the correlation coefficient (R). In this context, it was determined that the SC tool of the ANFIS resulted the wind speed predictions with the superior statistical error outcomes corresponding to 0.2562 MAE, 0.3047 RMSE, and 0.9990 R .

Keywords – Machine Learning, Long-Short Term Memory, Adaptive Neuro-Fuzzy Inference System, Wind Speed, Time-Series

I. INTRODUCTION

The power generation from renewable energy sources in all over the World is increasing recently due to the increase of global warming as well as the increase on the release of the greenhouse gases, and depletion of fossil fuels. Therefore, power plants operating with renewable sources have a significant spreading potential when compared according to the traditional fossil fuel power plants. Many countries of the World have this trend, and accordingly many countries in the World have at least one renewable type of power plant [1]. Among whole types of renewable power sources, wind technology is considered to be one of the most significant and extensive method of energy production. Fig. 1 presents World's cumulative installed wind power indicated according to the total onshore and offshore wind power plants. As demonstrated in this figure, the

analysis is provided considering the year ranges between 2001 and 2021 [2].

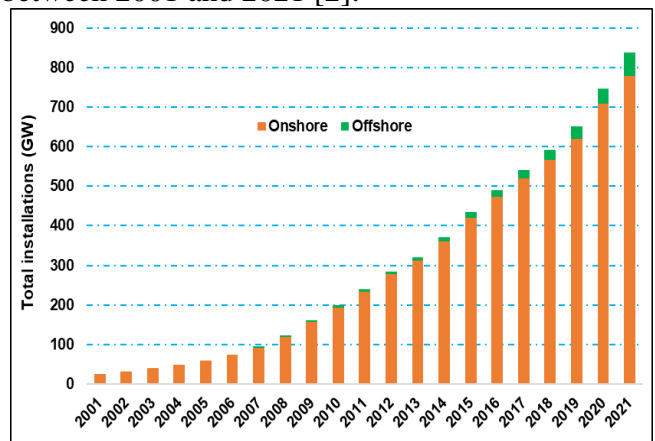


Fig. 1 Cumulative installations of wind power of the World

II. MATERIALS AND METHOD

A. Long-short term methods

An artificial recurrent neural network (RNN) is used in the deep learning architecture known as long short-term memory (LSTM). Unlike typical feedforward neural networks, LSTM has feedback connections. Both complete data sequences and lone data points can be handled by it [3-5]. For instance, the LSTM technique can be advantageous for tasks like connected, unsegmented handwriting identification, speech recognition, anomaly detection in network traffic, and IDSs (intrusion detection systems).

B. Adaptive Neuro Fuzzy Inference System (ANFIS)

The ANFIS architecture uses both ANN and fuzzy system (FS). The two systems work independently to achieve their own goals. The ANN can be used to increase the FS's adaptability to changing environmental conditions or to improve its parameters by reducing the difference between its output and a given specification. To improve precision and the output of the entire system, the output of an ANN is used to correct the output of an FS [6-10].

B1.Subtractive Clustering (SC) Algorithm

In this method, each data point is regarded as a prospective cluster center, and the potential of each data point is assessed by evaluating the density of data points surrounding the cluster center. Based on its placement in respect to other data points, this technique uses an adaptive process and assumes that any data point may be a cluster center [11].

B2. Fuzzy C-Means (FCM) Algorithm

The FCM approach identifies each data point's membership in relation to each cluster center based on the distance between the cluster center and the data point. Data is more likely to belong to a cluster center if it is located close to that center. Each data point's membership should add up to exactly one [10].

B3. Grid Partitioning (GP) Algorithm

The input data space is divided into rectangular grids by the GP algorithm. There is no physical or data density distribution behind the grid's creation. Based on system input-output data, the fuzzy rules are built using each grid segment, leading to rapid learning and shorter computation times [11].

C. Statistical Error Analysis

The mean absolute error (MAE), root mean square error (RMSE), and correlation coefficient (R) have all been used in this study as measures of statistical error. The better the outcomes, the closer the RMSE and MAE values are to 0. Besides, R values that are closer to 1, however, imply that the anticipated outcomes are more accurate and more correlated with the real values. The governing equations for MAE, RMSE, and R have been indicated in Eqs. (1), (2), and (3), respectively [1].

$$MAE = \frac{1}{N} \sum_{i=1}^N |p(i) - o(i)| \quad (1)$$

$$RMSE = \sqrt{\frac{1}{N} \sum_{i=1}^N [p(i) - o(i)]^2} \quad (2)$$

$$R = \frac{(\sum_{i=1}^N [p(i) - \bar{p}][o(i) - \bar{o}])}{(\sqrt{\sum_{i=1}^N [p(i) - \bar{p}]^2} \sqrt{\sum_{i=1}^N [o(i) - \bar{o}]^2})} \quad (3)$$

The abbreviations of i , N , $o(i)$, $p(i)$, \bar{o} , \bar{p} respectively, in the equations (1), (2), and (3) above, indicate the order of the data, the cumulative amount of the members of the considered data set, the real or field test data at a specific order, the machine predicted data at a specific order, the average of the real field test data, and finally average of the forecasted data [1].

III. RESULTS

This study was prepared using a total of 2,000 instantaneous wind speed data. While 80% of these total wind speed data was used to train machine learning that is corresponding to 1,600 wind speed data; the remaining 20% of the cumulative, were used to test the success of the simulations which is equal to 400 wind speed data. Accordingly, the computations are performed considering four algorithms of ANFIS-FCM, ANFIS-SC, ANFIS-GP as well as LSTM.

Considering the LSTM type of modelling, hidden layer for this algorithm is considered in between $5 \leq HL \leq 300$. Besides, the max. epoch number for the iterations has been adjusted to 300. On the other hand, in the FCM modelling of ANFIS, the number of the historical data required in training of the algorithm has been calibrated to stay in between $3 \leq HD \leq 10$, considering an increment of the $\Delta D = 1$, in this range of interval. The number of the membership functions, on the other hand, has been arranged in between $2 \leq MFs \leq 10$, with the increment in the computations of

$\Delta MFs = 2$. In SC algorithm of the ANFIS, the historical data required for training is adjusted in between the same range as in the case of FCM. The influence radius required in this algorithm is adjusted in the range of $0.2 \leq IR \leq 0.9$. Finally, in GP of ANFIS, while the HD is considered in between $3 \leq HD \leq 4$, the number of MFs has been studied in between $2 \leq MFs \leq 4$.

Among the considered algorithms, a total of 9 models have been investigated in LSTM modelling, a cumulative of 40 models have been examined in FCM tool of ANFIS, 48 models in total have been studied in SC approach, and finally, 5 models have been researched in GP algorithm. In this context, a total of 102 models have been formed and the statistical accuracy results depending on MAE, RMSE, and R have been revealed. Accordingly, the results of LSTM modelling have been shown in Table 1. On the other hand, the outcomes of ANFIS-FCM have been given in Table 2. Finally, the statistical accuracy results of SC and GP algorithms have been presented in Tables 3 and 4, respectively. The setting parameters of these algorithms have been also demonstrated in these tables.

Table 1. The results of LSTM computations

Hidden layer	Max. Epoch	MAE	RMSE	R
5	300	0.3170	0.3866	0.9967
10	300	0.3322	0.4159	0.9960
25	300	0.4180	0.5630	0.9894
50	300	0.6364	0.8347	0.9735
75	300	0.4989	0.6365	0.9853
100	300	0.5829	0.7707	0.9785
125	300	0.7981	1.1981	0.9398
150	300	1.4633	1.9753	0.8272
300	300	1.6805	2.3523	0.7658

Table 2. The results of FCM computations

Historical data	MFs	MAE	RMSE	R
3	2	0.2789	0.3406	0.9977
3	4	0.2972	0.3648	0.9969
3	6	0.2995	0.3730	0.9961
3	8	0.3353	0.4356	0.9939
3	10	0.3275	0.4354	0.9936
4	2	0.2888	0.3476	0.9976

4	4	0.3031	0.3758	0.9962
4	6	0.3236	0.4076	0.9950
4	8	0.3400	0.4720	0.9919
4	10	0.3605	0.4838	0.9917
5	2	0.2926	0.3558	0.9973
5	4	0.3337	0.4203	0.9953
5	6	0.3583	0.4522	0.9935
5	8	0.3789	0.4867	0.9916
5	10	0.4098	0.5419	0.9882
6	2	0.2987	0.3679	0.9971
6	4	0.3279	0.4208	0.9951
6	6	0.3794	0.4529	0.9939
6	8	0.4145	0.5240	0.9908
6	10	0.4181	0.5265	0.9901
7	2	0.3045	0.3764	0.9970
7	4	0.3240	0.4109	0.9955
7	6	0.4110	0.5030	0.9913
7	8	0.4671	0.4671	0.9912
7	10	0.4383	0.5641	0.9888
8	2	0.3121	0.3832	0.9968
8	4	0.3478	0.4357	0.9946
8	6	0.3907	0.4762	0.9929
8	8	0.4005	0.4863	0.9926
8	10	0.4421	0.5599	0.9884
9	2	0.3095	0.3836	0.9967
9	4	0.3481	0.4307	0.9949
9	6	0.4243	0.5226	0.9912
9	8	0.4223	0.5194	0.9914
9	10	0.5043	0.6549	0.9847
10	2	0.3015	0.3629	0.9970
10	4	0.3401	0.4196	0.9951
10	6	0.4307	0.5240	0.9910
10	8	0.4817	0.5883	0.9882
10	10	0.4986	0.6272	0.9862

Table 3. The results of SC computations

Historical data	IR	MAE	RMSE	R
3	0.20	0.2697	0.3593	0.9967
3	0.30	0.2647	0.3309	0.9975
3	0.40	0.2865	0.3886	0.9966
3	0.60	0.2664	0.3254	0.9982

3	0.80	0.2663	0.3209	0.9986
3	0.90	0.2562	0.3047	0.9990
4	0.20	0.3389	0.4214	0.9943
4	0.30	0.3077	0.3789	0.9964
4	0.40	0.2932	0.3613	0.9969
4	0.60	0.3009	0.3824	0.9971
4	0.80	0.2819	0.3372	0.9981
4	0.90	0.2640	0.3132	0.9987
5	0.20	0.4208	0.5507	0.9884
5	0.30	0.3582	0.4488	0.9945
5	0.40	0.3545	0.4383	0.9949
5	0.60	0.3144	0.3954	0.9965
5	0.80	0.2933	0.3576	0.9977
5	0.90	0.2910	0.3543	0.9979
6	0.20	0.4430	0.5669	0.9878
6	0.30	0.3707	0.4585	0.9941
6	0.40	0.3350	0.4228	0.9952
6	0.60	0.2985	0.3631	0.9973
6	0.80	0.2946	0.3590	0.9975
6	0.90	0.2911	0.3541	0.9977
7	0.20	0.3307	0.4241	0.9958
7	0.30	0.3575	0.4378	0.9945
7	0.40	0.3244	0.4126	0.9957
7	0.60	0.3033	0.3736	0.9971
7	0.80	0.2946	0.3599	0.9976
7	0.90	0.2935	0.3578	0.9977
8	0.20	0.4290	0.5709	0.9886
8	0.30	0.3790	0.4675	0.9927
8	0.40	0.3826	0.4536	0.9952
8	0.60	0.3064	0.3750	0.9971
8	0.80	0.3318	0.4089	0.9965
8	0.90	0.2962	0.3585	0.9976
9	0.20	0.5181	0.6726	0.9843
9	0.30	0.4436	0.5441	0.9906
9	0.40	0.4194	0.5042	0.9933
9	0.60	0.3453	0.4156	0.9959
9	0.80	0.3041	0.3708	0.9971
9	0.90	0.2930	0.3526	0.9976
10	0.20	0.5931	0.7939	0.9744
10	0.30	0.4851	0.6128	0.9872
10	0.40	0.3811	0.4673	0.9935
10	0.60	0.3370	0.4132	0.9957

10	0.80	0.3036	0.3721	0.9969
10	0.90	0.2944	0.3566	0.9974

Table 4. The results of GP computations

Historical data	MFs	MAE	RMSE	R
3	2	0.2643	0.3537	0.9973
3	3	0.3619	1.0333	0.9565
3	4	0.2643	0.3537	0.9973
4	2	0.3110	0.4285	0.9942
4	3	0.4624	1.4843	0.9186

In the predictions, the real data is discretised into two parts as demonstrated in Fig. 2. The blue part given alone and shown on the left indicates the data utilized for training of the algorithm. Whereas, the dashed red part coincident with the continuous blue on the right shows the predicted data obtained in the test part of the computations. Approximately, 80% and 20% of the total data are discretised respectively for training and testing of four algorithms. In the training stage, the computer develops the proper learning algorithm to obtain predictions presented in the right dashed red section coincident with the continuous blue part. In short, the real data function is exhibited with continuous blue colour, whereas the prediction data function is given with dashed red colour.

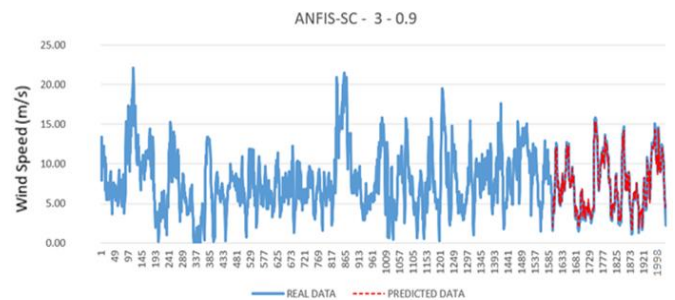


Fig. 2 The data pair of the real observed and predicted values of ANFIS-SC obtained at 3 HD and 0.90 IR

The best result of all 102 computations is obtained with SC of ANFIS at 3 HD and 0.9 IR. On the other hand, the best result of LSTM, FCM, SC, and GP are indicated with bold colour respectively in Tables 1, 2, 3, and 4. And, these best results are given in Table 5. Besides, the statistical accuracy results of the best result of the best outcomes of four algorithms, i.e., the result obtained at 3 HD and 0.90 IR of SC is exhibited with bold colour in Table 5. In this model, the

computation generated 0.2562 m/s MAE, 0.3047 m/s RMSE, and 0.9990 R.

Table 5. Statistical accuracy results of the best results

Model	MAE	RMSE	R
ANFIS-FCM	0.2789	0.3406	0.9977
ANFIS-GP	0.2643	0.3537	0.9973
ANFIS-SC	0.2562	0.3047	0.9990
LSTM	0.3170	0.3866	0.9967

Similarly, the second best result that is obtained by FCM of ANFIS at 3 HD and 2 MFs which is given in Table 2 is shown in Fig. 3. Both Figs. 2 and 3 indicate the high accuracy and success that are obtained in predictions by SC and FCM tools of ANFIS.

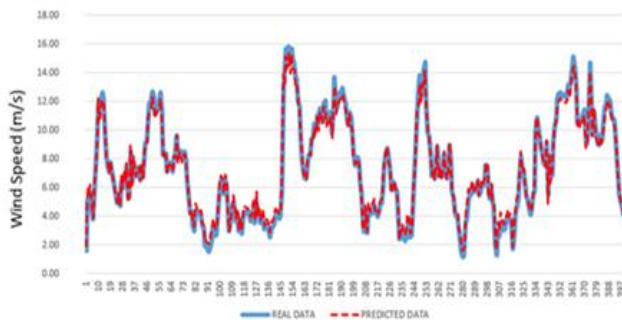


Fig. 3 The predictions obtained by FCM at 3 HD and 2 MFs

Figs. 4 and 5 give the correlation coefficient (R^2) results respectively for SC and FCM tools of ANFIS. In these figures, while the x axis stands for the real data cloud, whereas the y axis corresponds to prediction data cloud. Similarly, the correlation coefficient results for both algorithms show the wind speed predictions are enough compatible and coincident with their real counterparts. For SC and FCM algorithms, as shown in these figures, 0.9979 R^2 and 0.9982 R^2 are respectively obtained.

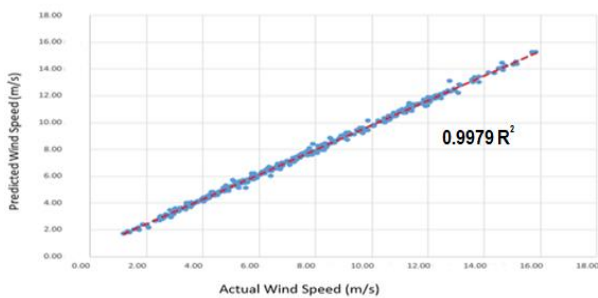


Fig. 4. The correlation results of SC of ANFIS

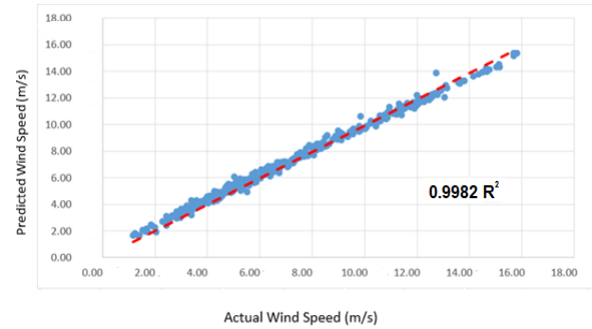


Fig. 5. The correlation results of FCM of ANFIS

IV. DISCUSSION

Today, physical data estimation has gained a lot of importance. For instance, wind speed estimation is among the most important of these physical data predictions. It is possible with machine learning to predict the future wind speed situation with only the historical time series wind data at hand, without the further need of any technical detailed knowledge or field experimentation. Thus, in this way, it is likely to get an idea about the future state of the wind speed parameter, which is the most important parameter that is greatly influencing the wind output power of the wind turbine.

V. CONCLUSION

In this study, the computations performed with the designed 102 models have indicated that the predictions have been generally performed with low margins of statistical errors. Especially, the computations performed using SC and FCM tools of ANFIS have indicated both tools can be safely applied in predictions of highly fluctuating wind speed data.

REFERENCES

- [1] A. Ilhan, "Forecasting of river water flow rate with machine learning," *Neural. Comput. Appl.*, vol. 34(22), pp. 20341–20363, Nov. 2022.
- [2] (2020) Global Wind Energy Council website. [Online]. Available: <https://gwec.net/>
- [3] S. Hochreiter and J. Schmidhuber, "Long short-term memory," *Neural Comput.*, vol. 9(8), pp. 1735-1780, Nov. 1997.
- [4] S. Zahroh, Y. Hidayat, R. S. Pontoh, A. Santoso, and A. T. Sukono Bon, "Modeling and forecasting daily temperature in Bandung," in *Proc. First GCC International Conference on Industrial Engineering and Operations Management*, 2019, pp. 406–412.
- [5] A. G. Salman, Y. Heryadi, E. Abdurahman, and W. Suparta, "Single layer & multi-layer long short-term memory (LSTM) model with intermediate variables for weather forecasting," *Procedia Comput. Sci.*, vol. 135, pp. 89-98, 2018.

- [6] H. Z. Abyaneh, A. M. Nia, M. B. Varkeshi, S. Marofi, and O. Kisi, "Performance evaluation of ANN and ANFIS models for estimating garlic crop evapotranspiration," *J. Irrig. Drain. Eng.*, vol. 137, pp. 280-286, May 2011.
- [7] J. R. Jang, "ANFIS: adaptive-network-based fuzzy inference system," *IEEE Trans. Syst. Man. Cybern.*, vol. 23(3), pp. 665–685, 1993.
- [8] O. Karakus, E. E. Kuruoglu, and M. A. Altinkaya, "One-day ahead wind speed/power prediction based on polynomial autoregressive model," *IET Renew. Power Gener.*, vol. 11(11), pp. 1430–1439, Sep. 2017.
- [9] H. Tabari, O. Kisi, A. Ezani, and P. H. Talaei, "SVM, ANFIS, regression and climate based models for reference evapotranspiration modeling using limited climatic data in a semi-arid highland environment," *J. Hydrol.*, vol. 444-445, pp. 78-89, Jun. 2012.
- [10] (2020) Mathworks Long Short-term Memory Networks website. [Online]. Available: <https://www.mathworks.com>
- [11] K. Benmouiza and A. Cheknane, "Clustered ANFIS network using fuzzy c-means, subtractive clustering, and grid partitioning for hourly solar radiation forecasting," *Theor. Appl. Climatol.*, vol. 137, pp. 31-43, 2019.